This is a repository copy of *A method for low-cost, low-impact insect tracking using retroreflective tags*.

White Rose Research Online URL for this paper:
https://eprints.whiterose.ac.uk/177556/

Version: Accepted Version

A method for low-cost, low-impact insect tracking using retroreflective tags

Michael Thomas Smith[*]   Michael Livingstone [†]   Richard Comont [‡]

Abstract

1. Current methods for direct tracking of individual bee movement behaviour have several limitations. In particular, the weight and size of some types of electronic tag may limit their use to larger species. Radars and other electronic systems are also often large and very expensive to deploy. A tool is needed that complements these electronic-tag methods. In particular one that is simple to use, low-cost, can have a high spatial resolution and can be used with smaller insects.

2. This paper presents a candidate method that uses retroreflective tags. These are detected using a camera with a global electronic shutter, with which we take photos with and without a flash. The tags can be detected by comparing these two photos. The small retroreflective tags are simple and light-weight, allowing many bees to be tagged at almost no cost and with little effect on their behaviour.

3. We demonstrate this retroreflector-based tracking system (RTS) with a series of simple experiments: Training and validation with a manually positioned tag; case studies of individual bees; tracking multiple bees as they forage in a garden; use of real-time monitoring to allow easy re-observation to enable a simple floral preference experiment; and a very brief experiment with 3D path reconstruction (integrating two devices). We found we could detect bees to a range of about 35 m with the current configuration.

4. We envisage the system will be used in future to increase detection rates in mark-re-observation studies; provide 3D flight path analysis; and for automated long-term monitoring. In summary, this novel tracking method has advantages that complement those of electronic-tag tracking which we believe will lead to new applications and areas of research.

Keywords: bee, flight path, foraging, insect, reobservation, retroreflector, tagging, tracking.

[*]Department of Computer Science, University of Sheffield, `m.t.smith@sheffield.ac.uk`
[†]Department of Landscape Architecture, University of Sheffield, `MILivingstone1@sheffield.ac.uk`
[‡]Bumblebee Conservation Trust, `richard.comont@bumblebeeconservation.org`

1 Introduction

Tracking individual bees in the wild can provide ecologists and neuroethologists with valuable information, helping them, for example, to investigate foraging (Saville et al., 1997), search strategies (Reynolds et al., 2007), orientation flights (Capaldi et al., 2000) and other aspects of cognition (Capaldi and Dyer, 1999) and can help researchers find nests (Kennedy et al., 2018). Our ability to track and detect individuals as they forage and explore the landscape is fundamental to our understanding of bee behaviour and ecology. The aim of this work is to provide a simple, low-cost, low-impact method for precision tracking of bees in the field.

We briefly review current methods for insect tracking, to motivate this paper's approach. We set aside indirect methods, such as 'mark and recapture'. Although the most simple, it is reportedly often biased by the location of the observers (Schaffer, 1997) and suffers from very low detection rates, due to the size of the foraging area involved (Schaffer, 1997). We instead focus on direct-tracking methods.

Azimuthally-scanning harmonic radar has been used to track flying insects for over twenty years (e.g Osborne et al., 1999; Charvat et al., 2003; Cant et al., 2005; Wolf et al., 2014; Milanesio et al., 2016) and has been vital for many discoveries, from forage search strategies (Reynolds et al., 2007) to orientation flights (Capaldi et al., 2000). These results were achieved due to its impressive range of several hundred metres (Osborne et al., 1996). See Riley and Smith (2002) for more technical details of its design. The technique's main shortcoming is that the equipment is very large, very expensive[1] and bespoke, making it inaccessible to most researchers (O'Neal et al., 2004), particularly in low-income countries. Precision typically is of the order of several metres (Cant et al., 2005), which is not sufficient for some applications. Low-power, mobile, direction-only detectors (e.g. using the popular Recco Rescue System, http://www.recco.com/) have also been used, with range reported as 13 m (Lövei et al., 1997), 40 m (Langkilde and Alford, 2002), 50 m (Roland et al., 1996) or 60 m (Psychoudakis et al., 2008). On tag size: Osborne et al. (1996) were able to tag and track *Apis mellifera* with 12 mg tags, and Chapman et al. (2004) report that 1 mg tags have been used to track tsetse flies.

Very high frequency (VHF) **radio transmitters** have also been used to track bumblebees (and butterflies) over even larger ranges than harmonic radar (Hagen et al., 2011; Fisher et al., 2020), with the support of a light aircraft. This approach requires a battery powered (200 mg) transmitter to be attached to the bee, leading to significant effects on bee behaviour (Hagen et al., 2011) and largely impossible to use with many insects. For comparison, the median weight of *Bombus terrestris* subsp. *audax* workers is only about 250 mg (Connolly and Moffat, 2015). Many of these electronic direct-tracking methods require an antenna to be attached to the insect, making it difficult to use with smaller insects, or those which need to access narrow spaces (such as burrowing insects or those which enter sympetalous flowers).

Other methods: Radio-frequency identification (RFID) tags have also been used, although these typically require the insect to be within 3 cm of the sensor (Nunes-Silva et al., 2019). Another recent electronic-tag alternative,

---

[1]STOPVESPA (2019, p31) suggest it cost their project €100,000 to construct.

with energy harvested from the insect's wing beats has been developed. This still has a somewhat heavy and complicated payload for the insect to carry (Shearwood et al., 2017), and has a range similar to the method described in this paper. Others have used lidar to track untagged bees (Bender et al., 2003) although this requires a very carefully prepared site and does not allow individual targets to be tracked. Abdel-Raziq et al. (2021) suggest the orientation of the sun could be used to infer flight path using an on-board sensor, using dead-reckoning, although the paper only has simulated data. Non-electronic tags have been used with other insects: Chemiluminescent tags have been used in dark environments (Spencer et al., 2017), and metal foil and metal detectors (Piper and Compton, 2002) for hidden insects.

A few previous papers have used **retroreflective tags** to track insects: Rennison et al. (1958) used reflective paints to search for Tsetse flies, at night, using a torch. Riley and Edwards (1994) experimented with retroreflective tags for green leafhoppers (*Nephotettix* spp.) in an unlit indoor test. Zanen and Cardé (1999) used them in a wind-tunnel to track the orientation of gypsy moths. Recent work explores the potential to use retroreflectors (at very close range) to image the insect using lasers and galvanometer motors (Vo-Doan and Straw, 2020).

In this paper we describe a low-cost method for detecting and tracking insects in the field using small retroreflective markers. Unlike the above cited retroreflector papers, we use a camera with a global electronic shutter and a flash: enabling it to work in sunny conditions and work over a greater range. The light-weight, simple tags mean there is likely to be less impact on bee behaviour than the electronic tags mentioned earlier. The range is limited to about 35 m line-of-sight, so we do not envisage it being a complete replacement for harmonic radar and VHF radio tracking, but anticipate it can provide a very useful method in the ecologist's toolkit. For example, the imaging accuracy can allow the precise flower being visited to be identified. A few example applications include: tracking bees that are potentially too small for electronic tagging, supporting re-observation studies to increase re-observation rates, 3D flight path analysis, and for automated long-term monitoring and tracking. We anticipate further applications to develop as the method matures.

2   Materials and Methods

2.1   Overview

The Retroreflector-based Tracking System (RTS) was developed using commercially available components and is simple to construct. The onboard software required is provided as open source python modules. See the supplementary for details.

Its operation is simple: A camera and flash are mounted on an elevated platform. Pairs of photos are taken, with and without the flash. A retroreflector attached to the bee reflects the flash's light back towards the camera. The non-flash photo is subtracted from the flash photo. A bright dot will remain on the photo after the subtraction,

indicating where the retroreflector is. This bright dot can be followed if multiple photo-pairs are taken. Various additional steps, described later, are required to reduce the false positive rate. This algorithm is run in real-time on the system's onboard raspberry pi computer, and the results are both saved internally and made available via a web interface hosted onboard allowing the field-worker to find the detected bee in real-time (using a mobile phone's browser, for example).

2.2 Bee Capture and Tagging

Over the course of the project we successfully tagged over 100 bees, and found this of similar technical difficulty to tagging in normal reobservation studies. After capture we used cold-induced narcosis to immobilise the bees for tagging (see Supplementary for more details).

We used a retroreflector with fabric substrate (from a hi-vis jacket) and cut it approximately to 8×4mm (we adjust the size depending on the size of the insect). This weighed about 5 mg.[2] Using tweezers we folded it in half and spread the ends of the two halves apart, so the reflector has a small ridge. This helped the RTS detect the bee from a wider range of angles. Using tweezers to hold the reflector by the ridge we applied a small amount of cyanoacrylate adhesive (Loctite superglue) to the reflector and affixed it to the thorax of the insect. We cut small notches in each tag prior to attachment, to allow later unique reidentification of each bee by a human observer.

The species of wild bees were identified during tagging by the field-worker (using Edwards and Jenner, 2018) and later confirmed (from photos) by the other authors.

2.3 The System

Several iterations of the RTS have been constructed. Here we describe the most advanced. The system's overall cost was about £820, of which £630 was the camera and lens (2020 prices). Figure S1a in the supplementary illustrates the prototype used.

Computer The system used a raspberry pi for controlling the flashes and camera and for processing and saving the camera output (Pi 4 model B, Raspberry Pi Foundation).

Camera and Lens The most important aspect of the camera (the monochrome 2064×1544 GCC2062M, smartek) was that it must have a global electronic shutter. This allowed for very brief exposures (e.g. 25 μs) just covering the duration of the flash. A standard machine vision 2 megapixel lens was used (Kowa LM5JCM 2/3" 5 mm F2.8 C-mount, Kowa American Corp.)

Flash Two or four flashes were used (TT560, Neewer, set to 1/16 power), either configured to fire in unison or sequentially. In the former the flash power was greater, thus potentially increasing the range of the system, but in the latter the system could take more photos as the flashes could sequentially recharge.

---

[2]This can be made lighter if required by removing the fabric on the reverse of the reflector.

2.4 Algorithm and Software

2.4.1 Overview

To find a retroreflective tag in the photographs requires some image processing. At its simplest, the algorithm needs to (a) align the flash and no-flash photos together, (b) subtract the no-flash photo from the flash photo, (c) find the brightest point. This simple algorithm is fairly successful, however we found false positives were being frequently detected. For a reobservation study in which a true positive is relatively rare, the false positive rate needs to be very low to avoid masking the rare true positive events.

We found false-positives (FPs) had a variety of causes. The most common were moving bright objects or features. These include the pattern of leaves and branches moving against the relatively bright sky leading to bright dots appearing and disappearing regularly in the subtracted image. Similarly reflective objects such as lamp posts, plant pots etc, often had reflections which led to bright pixels in the subtracted image. Humans or other animals moving within the scene could also lead to differences in the flash/no-flash photos. We also found occasional near-camera (out of focus) particles (possibly wind-carried seeds or pollen) were being brightly illuminated by the flash.

A three stage approach was taken to remove various types of FP event. First, rather than just subtract the non-flash photo, this photo is maximum-dilated (see supplementary) to ensure that small movements in the location of bright spots will still lead to them being cancelled in the flash photo. For example, a bright flower moving in the wind, or the dots of sky visible through a tree, can move between the two photos. The camera itself may also move slightly. By dilating the no-flash photo these bright dots will still be subtracted from their counterparts in the flash photo.

Second, some objects such as litter, a swinging bird-feeder, street signs, or other reflective objects do produce a bright reflection, which will appear in the flash/no-flash subtracted image. We handle this by noting that foraging bees rarely remain in the same location for long. Thus by combining (finding the maximum of) previous flash/no-flash subtractions, and then subtracting *this* from our current flash/no-flash image, we remove all the stationary sources of reflection.

Third, some objects may still appear, even in this resulting image. Examples include motes of pollen or wind-transported seed, or other moving retroreflectors such as car number plates etc. The retroreflective tag is far smaller than a pixel so leads to a very concentrated bright 'blob' of just a few pixels. Most other false positives that remain at this point are typically considerably larger. We use a machine learning classifier to identify and remove these remaining false positive targets.

2.4.2 Classifier Training

To collect training and validation data, we visited two locations (and used several camera orientations) over five days. We used a retroreflector on the end of a one-metre bamboo cane. We took photos of the reflector at various

distances up to 40 m, holding the reflector at different heights. We labelled 812 images. In each we specified the location of the retroreflector (easily identified as we could visually inspect the image and find the field-worker holding the cane). We also automatically found another 7,000 maximums in the difference images that were not the retroreflector. We then used six features (see below) associated with each of these points to train a (linear kernel) support vector machine (Chang and Lin, 2011) to distinguish between the two classes.

2.4.3 The Algorithm

The algorithm for detecting the tag in the photos consists of the following steps:

1. Capture: Regularly (between every 0.25 to 6 seconds) a set, S_i, of photos are taken. These sets we index: $i = 1..n$. We assume we are searching for the bee in the latest set, S_n. Within each set, S_i, there is one photo with the flash (F_i) and at least one without ($NF_i^{(1)}, NF_i^{(2)}...$). These are typically all taken within 2 ms of each other. We typically take the no-flash photo(s) first (to ensure the flash is not lit). Later, during analysis, we found a single no-flash photo was sufficient.

2. Alignment: A coarse or approximate alignment may be necessary within and between pairs of images if the RTS' platform is not stable (for example on the tethered balloon). This can be done using a standard library (OpenCV) or for translation-only we found a convolution of a low-resolution version of the image provided very fast coarse-alignment.

3. Subtraction (for current set S_n): For the current set, S_n, we maximum-dilate, $D_M(\cdot)$, (see supplementary) each of the non-flash photos, which is then subtracted from the flash photo. The minimum pixel values, A_n, over these subtracted pairs is computed (where the min operator is per pixel), so for pixel k, $[A_n]_k = \min_j \left[[F_n - D_M(NF_n^{(j)})]_k \right]$

4. Subtraction (for all previous sets S_i, $i \in 1..n-1$): For each previous set, S_i, we do not dilate either image, we just subtract each of the non-flash photos from the flash photo. The *maximum* pixel values, B_n, over all these subtracted pairs, from all the previous sets, is computed (where the max operator is per pixel), so for pixel k, $[B_n]_k = \max_{i \in 1..n-1} \max_j \left[[F_i - NF_i^{(j)}]_k \right]$. The maximum per set can be cached as it is used repeatedly.

5. Overall subtraction: We apply the maximum-dilate operation to the maximum subtraction image, B_n, from the previous sets and subtract this from the current difference image to give us our resulting search image, $R_n = A_n - D_M(B_n)$.

6. Finding Candidate Patch Features: We now find the brightest points in the search image. We iteratively find the location of the maximum pixel p in R_n: $p = \text{argmax}_k [R_n]_k$. For this maximum point we record six features:

    - The value of the maximum, $[R_n]_p$

- The value of the maximum pixel from $F_n - NF_n^{(1)}$ in a 7×7 patch centred on the maximum pixel, p.

- The background mean: The average of the 40×40 patch surrounding the maximum pixel, p, excluding a central 7×7 square, from $F_n - NF_n^{(1)}$.

- The maximum of wider surrounding points: We find the maximum pixel value of 8 evenly-spaced pixels placed in an 8×8 square around p, from $F_n - NF_n^{(1)}$.

- The maximum of closer surrounding points: We find the maximum pixel value of 8 evenly-spaced pixels placed in an 4×4 square around p, from $F_n - NF_n^{(1)}$.

- Centre sum: The sum of pixel p and its four neighbours, from R_n.

These simple features are chosen to distinguish between true tags and other sources of maxima in the resulting image. These non-tags typically have a greater spatial extent which these heuristics are chosen to detect. We then delete a 15×15 square centred on p, and repeat the search for candidate patches. Typically we generate 20 candidate patches.

7. We finally use these six features to query a support vector machine classifier, previously trained on manually generated and labelled data. This gives a score/confidence for each of these candidate patches. We select a threshold depending on the application.

2.5 Applications

To provide a demonstration of the RTS being used, we ran a series of simple experiments.

The first, a simple tracking experiment, recorded the time bees were detected around different flower patches in a garden (Section 3.3.1).

In the second, we investigate floral preference (Section 3.3.2). Individual floral preference is a well known feature of *Bombus* sp. (e.g. Wilson and Stine, 1996). We wished to test whether or not individual bees have a preference for particular flowers in our study (compared to their species' average). When the system detected a bee, a field-worker found and identified the individual bee (and the flowers it was foraging on). Contingency tables were constructed for each species, to test for forage preference at the level of individuals.

In the third experiment, a 3D flight path reconstruction experiment was conducted (Section 3.3.3). A single RTS can only resolve a tag's location to a vector, which passes through the camera, and with a direction determined by the tag's position in the photo. If the same bee is tracked simultaneously using two tracking systems placed at different locations, the flight path of the bee can be reconstructed by combining this series of vectors. We provide more details of this approach in the supplementary.

2.6   Field Sites

For the evaluation phase we used Site A (53°22′16.6″ N, 1°30′49.7″ W) and Site B (53°22′16.7″ N, 1°30′45.1″ W). These are both on a quiet suburban private road in Sheffield, UK, with a backdrop of buildings, trees, parked cars and plants. We used these with the aim of providing a relatively challenging environment for the RTS during the evaluation. The tracking system was mounted approximately 1.5 m above the ground at these locations. The case studies were conducted at: Site C, an experimental ornamental urban meadow in Sheffield (53°22′46.2″ N, 1°26′09.7″ W); Site D, a small wild-flower area in part of the University of Sheffield's landscaped campus (53°22′17.9″ N, 1°30′26.1″ W); Site E, a garden on the edge of the small, rural town of Minchinhampton, Gloucestershire, UK (51°42′34.8″ N, 2°10′31.0″ W); Site F, a garden in the village of Chedworth, Gloucestershire, UK (51°47′51.2″ N, 1°55′03.7″ W). At Site D the tracking system operated resting on a step-ladder at the top of a bank, approximately 3 m above the height of the mini-meadow. At Site E we placed the tracking system on a flat roof, so it was raised approximately 2.5 m above the ground. At Site F it was placed on a step ladder (1.5 m above the ground).

The 3D reconstruction experiment, at Site G, was on a lawn at another part of the University of Sheffield campus, surrounded by trees and a nearby small allotment (53°22′21.5″ N 1°30′08.4″ W). The two tracking systems were approximately 1 m above the ground.

3   Results

3.1   Detection Range Evaluation

The supplementary includes both a calculation of the theoretical range and an empirical evaluation of tag detection for different distances, at Site A and Site B. To summarise, we found that the RTS worked to approximately 35 m. Using all four flashes and a threshold that achieved a false positive rate of zero (for the data collected) we detected 17/25 tags at 30 m and 1/18 tags at 39 m. These results are sensitive to the presence or absence of objects that generate false positives, the size and orientation of the reflector and the ambient daylight.

3.2   Case Studies

Before looking at tracking, floral preference and 3D trajectories, it is worth looking at the detection of single, tagged bees, as these case studies provide simple, clear examples of the utility of the RTS. Further discussion and results, including the use of a tethered balloon platform, are in the supplementary.

3.2.1   First field trial: Bumblebee re-observed in pine tree

Our first field trial (12:00-13:00 BST, 20 June 2020) with the current RTS was with a wild worker *Bombus terrestris* which we caught foraging in a mini-meadow area at Site D (Figure 1e). It was tagged (Figure 1a & 1b) and released.
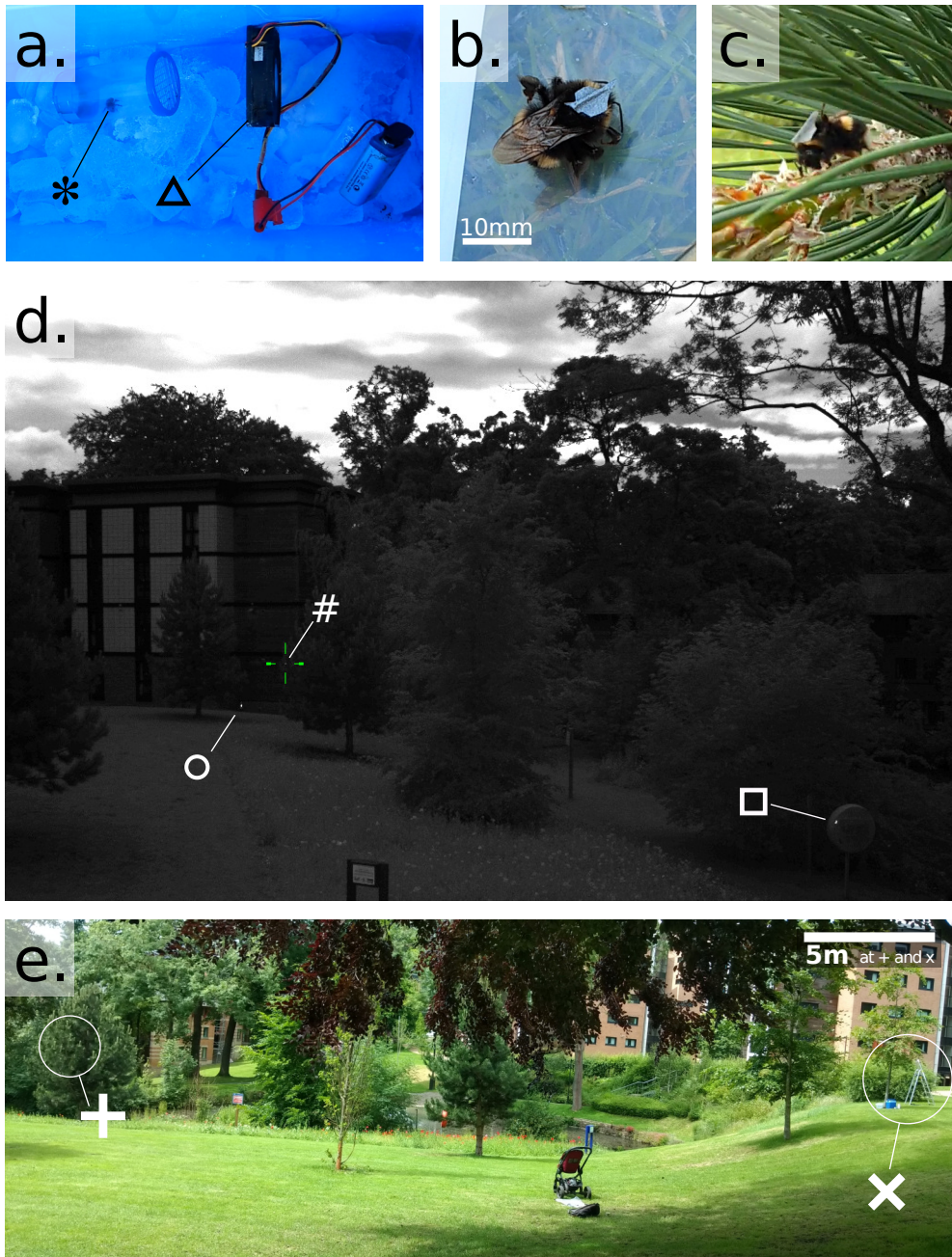
Figure 1: a. Tagging bees in the field using an icebox of salt/ice, a marking pot with mesh at both ends (∗) and an electric fan (△). b. Tagged *Bombus terrestris*. c. The same bee having been detected in the pine tree. d. Image from tracking system, with the bee detected (#) and examples of other reflections: a lifebuoy cover (□) and the retroreflective material on a traffic cone (○). e. The pine tree where the tagged bee was detected (+) and the tracking system (×).
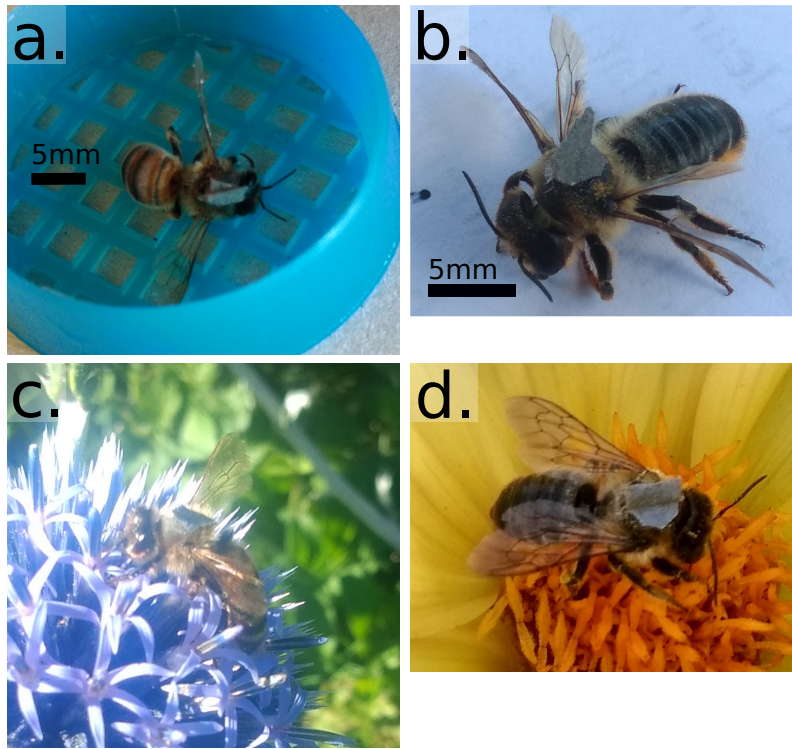
Figure 2: Newly tagged *Apis mellifera* (a) and *Megachile* sp. (b). c. The *Apis mellifera* later found foraging on a *Echinops ritro*. d. The *Megachile* sp. later found foraging on a *Dahlia* sp. flower.

We monitored the wild-flower area at the site, with the tracking system, anticipating the bee would return to the forage. However the system unexpectedly found it 3 m above the ground in a pine tree, 33 m from the tracking system (Figure 1c & 1d).

Figure 1d illustrates reflections from other objects (a lifebuoy cover and the retroreflective material on a traffic cone). Although both of these objects reflected the flash, they were stationary, and so were cancelled by subtracting previous image pair differences (step 5 in Section 2.4.3). They would also have been removed by the classifier due to their extent and shape.

3.2.2   *Megachile* sp. and *Apis mellifera* Tagged and Re-observed

In Sections 3.3.1 and 3.3.2 most of the bees tagged were *Bombus* spp., however (at Site E) we did also find and tag a *Megachile* sp., foraging on a yellow *Dahlia* sp. See Figure 2b. The floral preference experiment below involved using the tracking system to quickly find the tagged bees and then manually uniquely identify the individuals. On two occasions the tagged *Megachile* sp. was re-identified using the system, once on the same area of *Dahlia* as it was originally foraging on (Figure 2d), and once on a nearby *Verbena bonariensis*. This case study demonstrated that the retroreflectors can be used on smaller bees than *Bombus* spp. At Site F we tried tagging four *Apis mellifera* but with less success due to the species' relatively small thorax. However using the RTS we found one of them, 210 minutes later, foraging on the same patch of *Echinops ritro* that we caught it on originally (Figures 2a and 2c).
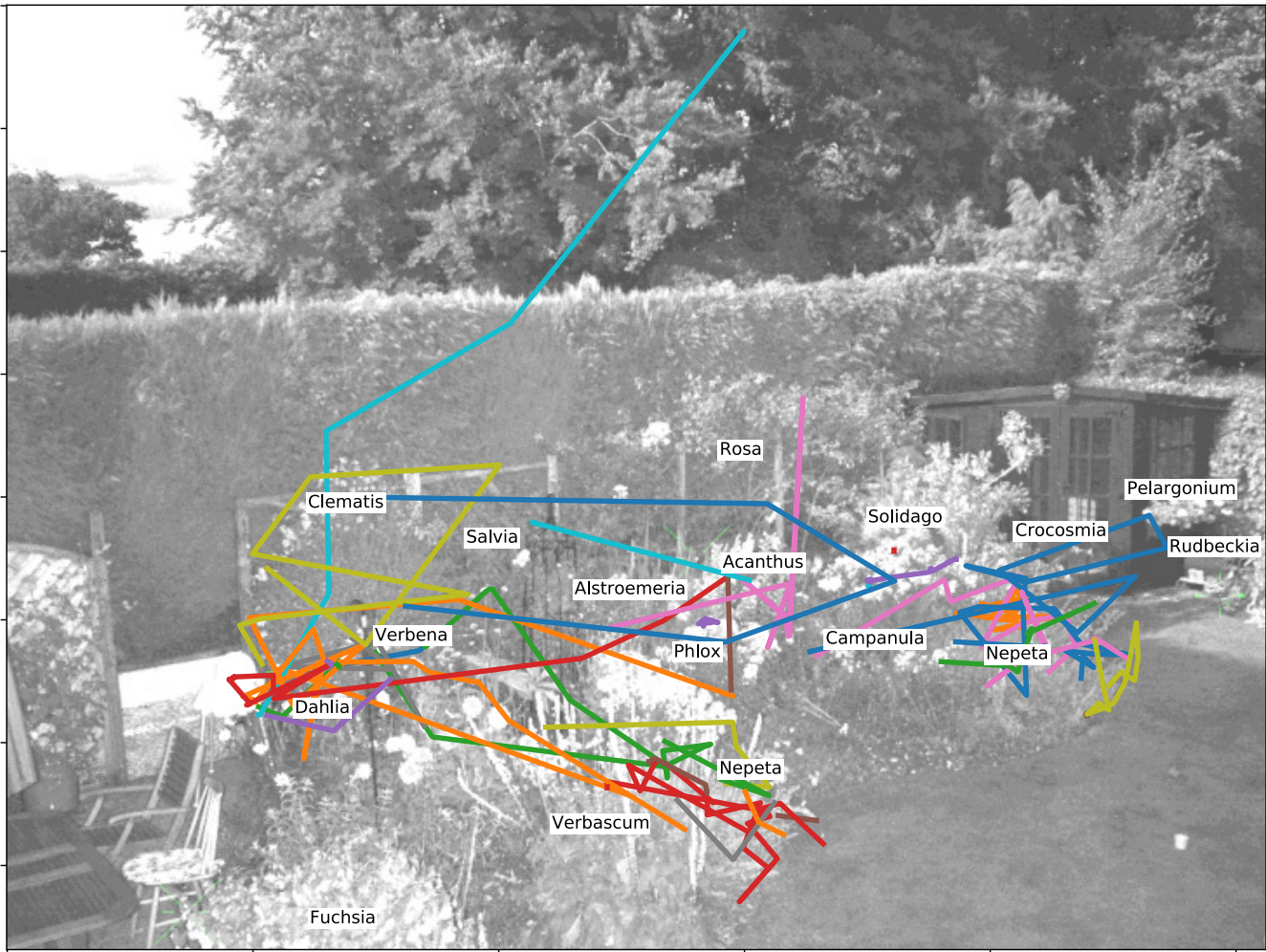
10

Figure 3: The paths of bees detected using the RTS. Each line represents one track (some colours may appear similar but this does not imply the bee was the same). Foraging area extended from 8 m to 15 m from the tracking system. The plants available for forage are labelled.

3.3 Applications

3.3.1 Tracking Foraging Bees

At Site E, we successfully tagged approximately 25 wild bees. They were caught and tagged largely at random, but with a slight selection preference towards tagging a variety of species (see Section 3.3.2 for species list). The tagging took place on 2 August 2020 and 3 August 2020. We ran the RTS on 2 August 2020 (cumulatively for 66 minutes between 11:36 and 19:04 BST), 3 August 2020 (for 82 minutes between 17:07 and 18:29 BST) and 5 August 2020 (cumulatively for 55 minutes between 11:57 and 14:15 BST). Most of this time it was being used to locate bees for the floral preference study (see Section 3.3.2) but data was recorded over a cumulative time of 3 hours, 23 minutes. In that time the system stored 1,303 flash photo pairs and acquired approximately 418 confirmed detections. These were semi-autonomously merged into 36 tracks (median length, 7 detections, min = 1, max = 45). These are plotted in figure 3. Some of the tagged bees will be responsible for several of these tracks. Besides

11

Plant	Detection events	Percentage	Normalised Percentage
Clematis	4	1%	2%
Rosa	2	1%	0%
Salvia	2	1%	1%
Solidago	10	3%	9%
Crocosmia	0	0%	0%
Pelargonium	1	0%	1%
Rudbeckia	0	0%	0%
Alstroemeria	2	1%	1%
Acanthus	15	5%	10%
Phlox	52	16%	22%
Verbena bonariensis	13	4%	9%
Campanula	2	1%	1%
Dahlia	64	19%	15%
Nepeta	139	42%	26%
Verbascum	25	8%	3%
Fuchsia	0	0%	0%

Table 1: Number of times a tag was detected in proximity to each flower species over the 3 hours 23 minutes. Normalising performed by dividing count by patch area in photo.

providing an example of how one can use the system for monitoring high-resolution foraging behaviour we also used the raw data to investigate the time spent on various foraging resources. Importantly this approach allows an automatic allocation of foraging time. We segmented the image into plant species. Figure 3 illustrates the plants available for forage and their locations. Table 1 shows the time spent on each plant type. We normalised by the visible area for each plant species. The results in the table suggest that there is a considerable preference for time spent foraging on Nepeta, Dahlia and Phlox.

3.3.2 Floral Preference

We ran a simple experiment over the three days to investigate floral preference (again using Site E). We left the system running over a cumulative 11 hours (intermittently from approximately 11:30 BST until 17:30 BST on each day). While it was running the field-worker was largely occupied by other activities, however, the system would alert him via a sound from the mobile phone web interface to the detection of a bee. The web interface would show a cross marking the recent location of the bee, allowing him to quickly find the bee and take photos (using a standard camera) for later unique identification (using the shape of the tag).

Overall 19 tagged bees were re-observed and identified using this approach, 50 times (nine *B. terrestris*, four *B. hortorum*, three *B. pascuorum*, one *B. lucorum/terrestris*, one *B. lapidarius*, one *Megachile* sp.), consisting of a mix of queens and workers. For each reobservation the unique bee and its forage were recorded. Not all bees were recorded that were detected - some left before the field-worker reached their location, or sometimes multiple bees were detected simultaneously.

We grouped those uniquely identified by species of bee, and constructed contingency tables (bee ID vs flower species, see Table 2). We excluded observations in which a previous observation for the same bee was within 10

	Bee Id.				
	#23	#30	#6	#7	
Fuchsia 'Garden News'	1	0	0	0	1
Nepeta sp.	0	0	2	1	3
Stachys byzantina	0	4	0	0	4
	1	4	2	1	8

	Bee Id.									
	#32	#1	#4	#36	#18	#21	#22	#27	#28	
Nepeta	5	0	0	0	1	0	0	1	0	7
Salvia 'Hot Lips'	0	0	0	0	0	0	0	0	4	4
Verbena bonariensis	0	0	0	0	0	1	0	0	0	1
Agapanthus africanus	1	1	0	0	0	0	0	0	0	2
Dahlia 'Bishop of York'	2	0	0	1	1	3	2	0	0	9
Stachys byzantina	0	0	1	0	1	0	0	0	0	2
	8	1	1	1	3	4	2	1	4	25

Table 2: Contingency tables for individual bee flower visits for *B. hortorum* (upper table) and *B. terrestris* (lower table). Other species had fewer than four visits each.

minutes, to avoid correlations due to temporal proximity. We wished to test whether bees have individual preferences for particular flower species. If individuals had no floral preference we would expect no interaction in the contingency table: the expected proportion of visits to a given flower should be the same for all unique bees (this was our null hypothesis). We note that in practice, preferences might be driven by caste, subspecies differences, or temporary environmental differences. However, as a simple test to demonstrate the RTS it should suffice.

Clearly the expected and observed numbers in the cells of these contingency tables are small, so the χ^2 test is inappropriate. We instead used the Exact Fisher Test.[3] We only had enough samples to perform this analysis for two species, We found for both *Bombus hortorum* ($p < 0.01$) and *Bombus terrestris* ($p < 0.001$) that there were significant individual preferences for particular forage species beyond that expected by chance (i.e. if the individuals of the same species had the same preference for each plant type).

3.3.3 3D flight trajectory

A final brief experiment used two RTS to compute the flight path of a bee (Figure 4b), to demonstrate this as a possible application. We used a single *Bombus terrestris* subsp. *audax* commerical nest (Biobest, standard hive, no cotton wool, containing about 80 workers) and tagged workers using the retroreflective tags. We placed the nest at Site G and positioned two RTS units facing the nest, approximately 15 metres from the nest and from each other. The nest had been open for a couple of days, so the workers had been foraging and had gained familiarity with the landscape. We started photographing with two RTSes as we saw workers depart (Figure 4d). The bee we successful tracked flew briefly North but turned South East (Figure 4a) and quickly accelerated (to a recorded speed of about 6 ms^{-1}), gradually climbing to an approximate height of 2.5 m (Figure 4c) before leaving the field of view of one of

---

[3]$M \times N$ contingency implementation thanks to Noutahi (2018), using Markov chain Monte Carlo (MCMC) sampling to compute the p-value.
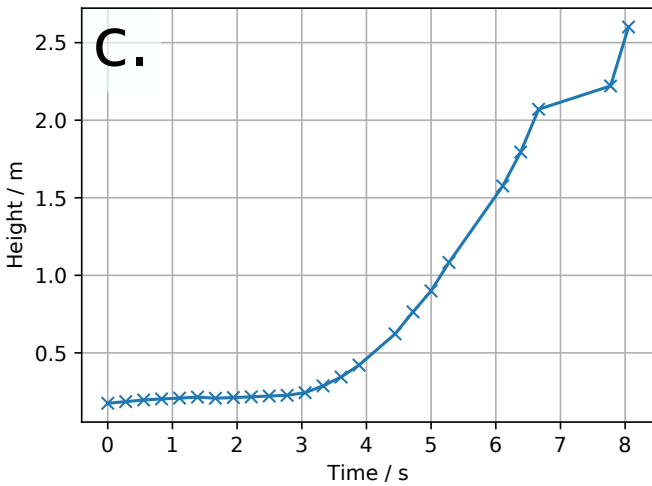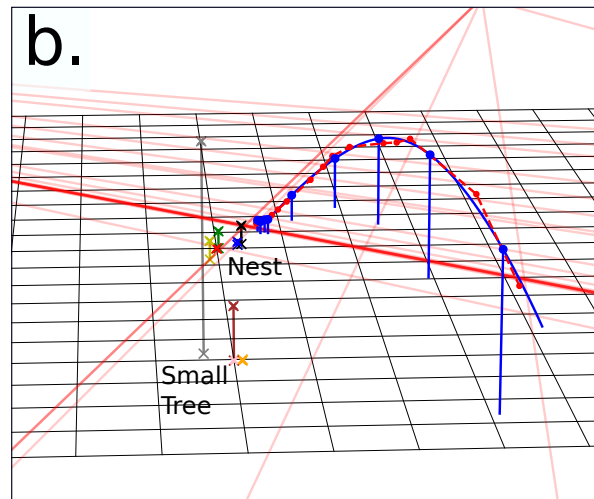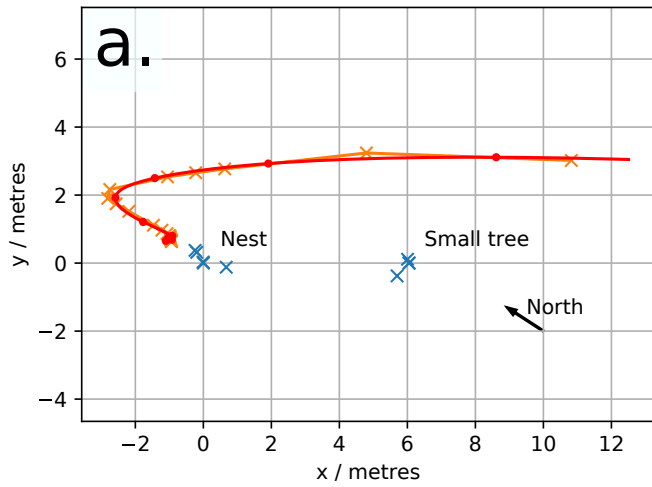
Figure 4: Reconstructed 3D flight trajectory. a. top-down projection of flight path. Orange line and crosses, the estimated observation locations. Red line and circles, fitted path with markers each second. Blue crosses, landmarks. b. 3D perspective projection. Dashed red line and circles, estimated observation locations. Blue line and circles, fitted path with markers each second. Crosses and vertical lines, various landmarks. Red lines indicate vectors centred on the two cameras, each associated with an observation. Ground plane grid squares 1×1 metres. c. Height of bee during flight. d. Photo taken from new pi 4 tracking system. The researcher and nest are in the foreground a tagged bee is illuminated and visible near the centre of the frame. The 'small tree' landmark is the tree to the right of the image.

14

the cameras. We failed to record other flights mainly due to problems with the nest (possibly due to the absence of cotton wool). This should be considered a proof-of-concept experiment.

4   Discussion

Researchers have developed several methods to directly track individual bees. Most of these methods use an electronic tag, either producing an active radio signal or passively providing a radar reflection. Retroreflective tags have also been explored, typically in dark environments and/or at close range. The RTS described in this paper works at greater range and in daylight, using such tags, thanks to two innovations. First is the use of a camera flash combined with a global electronic shutter. This massively reduces the ambient light detected while also providing a very powerful light source. Second is the algorithm devised to remove false positives by both comparing with previous photos and classifying using previous training data. The main disadvantage of the approach, compared to the radar and VHF tags, is the method's limited range of about 35 m. However, its advantages complement those methods: The system can provide very precise tracking data (in 2d or 3d) allowing visits to individual patches of flowers to be identified, for example. It is low cost compared to the other methods. Finally, the tag itself is very small and simple, and does not require the aerial of the electronic devices. In our brief experiment we found no evidence of behaviour change (although care must be taken if using cotton-wool as insulation in an artificial hive). The majority of bee species in the UK would probably find the electronic tags too cumbersome. Given that we were able to tag and track an *Apis mellifera*, it is likely that the retroreflective tag could be used with many other species of bee of around this size.

We found the initial experiment, tagging a forgaing *Bombus terrestris* (Section 3.2.1) and using the RTS to later detect the bee, was particularly convincing as to the method's effectiveness. The pine tree would not have been a location we would have looked for the bee, if trying to re-observe during a transect. Even if the bee had returned to the wild-flower area, finding it manually would have been laborious and unreliable. The simplicity and effectiveness of the detection demonstrates the benefits the system can bring to re-observation studies in particular.

The tagging of *Apis mellifera* and *Megachile* sp. in Section 3.2.2 demonstrate an important capability, as these are considerably smaller than the *Bombus* spp. tagged elsewhere. The smaller retroreflectors used do reduce detection range, but not as severely as one might expect. This we speculate is due to the $1/d^4$ relationship in signal strength. For example, the tag on the *Apis mellifera* probably has only 4 mm^2 visible, compared to a typical tag on a *Bombus* sp. that might have up to 20 mm^2 visible. The reduced size is equivalent in terms of simple signal strength to a 33 per cent reduction in distance (e.g. if the RTS works to 30 m with the large tag, it will work to about 20 m with the smaller tag). The *Apis mellifera* was detected approximately 16 m from the RTS, which fits this hypothesis.

Anecdotally, field studies often are limited by field-worker time. Section 3.3.1 demonstrated the system's

capability to perform detection and tracking automatically. To compare our results with anecdotal forage preference estimates, we asked the owner of the garden to recall the top three plant species over August 2020 they felt were most popular with bumblebees. They suggested: Nepeta, Dahlia and Verbascum. This fits quite closely with our results but with Phlox instead of Verbascum. This suggests that the automatic monitoring results reflect plausible foraging activities.

To move beyond single case-studies, we performed a simple floral preference experiment (Section 3.3.2) and demonstrated the automatic monitoring and tracking that the system can provide. We also demonstrated in a proof-of-concept experiment how one can combine data from two systems to infer the bee's flight path in 3D (Section 3.3.3).

There is a considerable range of experiments and research questions that could be supported with this technology, we just mention a few and then discuss future improvements to the underlying method.

4.1 Future Experiments

First, the most obvious initial use is as part of a standard mark-reobservation study, to increase the detection rate. The system could also be left to run autonomously for long periods, further increasing the rate of reobservation. Goulson (2003) wrote that 'In more typical, patchy landscapes the mark-reobservation method seems to be of little use without a huge team of observers to search for bees.' We propose that a small number of these tracking systems deployed at different locations can play the role of this 'huge team'.

Second, many bees only forage within 100-300 m of the nest (Gathmann and Tscharntke, 2002). Given the low cost of the tracking system, we envisage that one could monitor a useful portion of the foraging range of such doorstep foraging species, by distributing several tracking systems over much of the plausible area likely to be visited.

Third, we found the 3D path reconstruction was relatively simple to achieve with this system, and is likely to be a method of considerable interest to neuroethology, as it allows one to record in considerable detail initial learning flights, and investigate how modifications to the environment lead to changes in behaviour, allowing inference to be made around the cognitive processes involved in the bee's navigation and perception. Ideally more than two tracking systems should be used together, to further refine the path, and providing some redundancy to the data (see 'Tracking in three dimensions' on p420 in Dell et al., 2014; Straw et al., 2011).

Fourth, the RTS can remain in a fixed location, monitoring part of the landscape for considerable periods (with provision of electricity being its only limit). We suggest long-term floral preference studies could easily be conducted. We also noticed anecdotally that in our data we would often see several bees foraging at the same time, then have a period with none. We wonder if this is chance, or due to cyclic patterns in nectar depletion or possibly due to slight changes in the environment (temperature or wind). The high spatial resolution could also allow many individual flowers to be monitored for tagged bees, simultaneously.

Finally, the system's low cost, small size, ease of deployment and simplicity of use will give more researchers greater access to direct-tracking. For example, early nest finding could be achieved by tagging a foraging queen and tracking her back to the nest. One might best achieve this with the harmonic radar or VHF radio tags, but access and use of these tools is quite limited. Anecdotally we have noticed how queen bees, like workers, return on a similar path (or 'bee line') regularly to a forage patch. One could move or distribute the tracking system(s) along this path to eventually discover the nest.

4.2 Future Improvements

We first note that some simple hardware improvements, such as mounting on a rotating platform (which we experimented with previously) and using a slightly telephoto lens and a Fresnel flash lens could considerably increase the area scanned, potentially to about 1 hectare.

The next methodological improvement we are investigating is the potential for unique bee identification by combining the retroreflectors with colour filters to allow a colour camera to uniquely identify different tagged bees. Further refinement could be achieved by adding additional filters to the camera flashes. This will allow, for example, the floral preference study to have been run without field-worker intervention.

Although tagging bees with the retroreflective labels is relatively simple, it might be possible to tag all the bees using retroreflective powder, using the technology described in Osborne et al. (2008) for mass-marking.

The capacity to take 4 photos each second suggests that we should use the sequence of images to improve the detection and tracking accuracy (both in 2D and 3D). Future work should investigate the use of Bayesian approaches for such integration. A particle filter is probably an appropriate method as the dimensionality of the domain is low and the state space is non-linear with a multimodal posterior. In 3D the particle filter would be particularly effective as the likelihood function will consist of distributions along various vectors (each associated with a bright pixel in a photo).

Finally, building on our earlier work using alternative platforms, we found that, as the tracking system is fairly lightweight it can be used with drones, balloons and 10 m masts. Each of these has its own advantages, in particular one might envisage combining this with work such as Le et al. (2017), tracking the tagged bee with a unmanned aerial vehicle (UAV), allowing the evaluation of landscape features as corridors or barriers to bumblebees.

4.3 Conclusion

We have presented a novel method for tracking bees using small, light-weight retroreflective tags, using low-cost equipment. This method complements electronic and indirect tracking tools, for example it allows tracking of smaller bees than harmonic radar or VHF radio. We anticipate the Retroreflector-based Tracking System will support a wide range of ecological research.

Acknowledgements

Data Availability: Experimental data collected during the experiment has been archived (Smith, 2021c) in the University of Sheffield's Research Data Catalogue and Repository[4]: `https://doi.org/10.15131/shef.data.14650161`. Code: Two python modules have been written to collect and analyse the camera images in real-time, on-board the tracking system. The full code is available to download and use from `https://github.com/lionfish0/bee_track` (Smith, 2021b) and `https://github.com/lionfish0/retrodetect` (Smith, 2021a).

Conflict of Interest statement: The authors have no conflicts of interest.

References

Abdel-Raziq, H. M., Palmer, D. M., Koenig, P. A., Molnar, A. C., and Petersen, K. H. System design for inferring colony-level pollination activity through miniature bee-mounted sensors. *Scientific reports*, 11(1):1–12, 2021. doi: 10.1038/s41598-021-82537-1.

Bender, S. F. A., Rodacy, P. J., Schmitt, R. L., Hargis, P. J., Johnson, M. S., Klarkowski, J. R., Magee, G. I., and Bender, G. L. Tracking honey bees using LIDAR (light detection and ranging) technology. *Sandia Report SAND2003-0184*, 87185, 2003.

Cant, E. T., Smith, A. D., Reynolds, D. R., and Osborne, J. L. Tracking butterfly flight paths across the landscape with harmonic radar. *Proceedings of the Royal Society of London B: Biological Sciences*, 272(1565):785–790, 2005. doi: 10.1098/rspb.2004.3002.

Capaldi, E. A. and Dyer, F. C. The role of orientation flights on homing performance in honeybees. *Journal of Experimental Biology*, 202(12):1655–1666, 1999. doi: 10.1242/jeb.202.12.1655.

Capaldi, E. A., Smith, A. D., Osborne, J. L., Fahrbach, S. E., Farris, S. M., Reynolds, D. R., Edwards, A. S.,

---

[4]https://www.sheffield.ac.uk/library/rdm/orda

Martin, A., Robinson, G. E., Poppy, G. M., et al. Ontogeny of orientation flight in the honeybee revealed by harmonic radar. *Nature*, 403(6769):537–540, 2000. doi: 10.1038/35000564.

Chang, C.-C. and Lin, C.-J. LIBSVM: A library for support vector machines. *ACM Transactions on Intelligent Systems and Technology*, 2:27:1–27:27, 2011. doi: 10.1145/1961189.1961199. Software available at `http://www.csie.ntu.edu.tw/~cjlin/libsvm`.

Chapman, J. W., Reynolds, D. R., and Smith, A. D. Migratory and foraging movements in beneficial insects: a review of radar monitoring and tracking methods. *International Journal of Pest Management*, 50(3):225–232, 2004. doi: 10.1080/09670870410001731961.

Charvat, G. L., Rothwell, E. J., and Kempel, L. C. Harmonic radar tag measurement and characterization. In *IEEE Antennas and Propagation Society International Symposium. (Cat. No. 03CH37450)*, volume 2, pages 696–699. IEEE, 2003. doi: 10.1109/APS.2003.1219331.

Connolly, C. N. and Moffat, C. The number and individual weight of bumblebees (Bombus terrestris audax) from nests containing neonicotinoids in Wester Ross, UK. 2015. doi: 10.5285/341414f8-e88a-43e5-ade3-c30623c1586d.

Dell, A. I., Bender, J. A., Branson, K., Couzin, I. D., de Polavieja, G. G., Noldus, L. P. J. J., Pérez-Escudero, A., Perona, P., Straw, A. D., Wikelski, M., et al. Automated image-based tracking and its application in ecology. *Trends in ecology & evolution*, 29(7):417–428, 2014. doi: 10.1016/j.tree.2014.05.004.

Edwards, M. and Jenner, M. *Field Guide to the Bumblebees of Great Britain and Ireland New Revised Edition*. Ocelli; 6th edition, 2018.

Fisher, K. E., Dixon, P. M., Han, G., Adelman, J. S., and Bradbury, S. P. Locating large insects using automated VHF radio telemetry with a multi-antennae array. *Methods in Ecology and Evolution*, 2020. doi: 10.1111/2041-210X.13529.

Gathmann, A. and Tscharntke, T. Foraging ranges of solitary bees. *Journal of Animal Ecology*, 71(5):757–764, 2002. doi: 10.1046/j.1365-2656.2002.00641.x.

Goulson, D. *Bumblebees: Their Behaviour and Ecology*. Oxford University Press, USA, 2003.

Hagen, M., Wikelski, M., and Kissling, W. D. Space use of bumblebees (Bombus spp.) revealed by radio-tracking. *PloS one*, 6(5):e19997, 2011. doi: 10.1371/journal.pone.0019997.

Kennedy, P. J., Ford, S. M., Poidatz, J., Thiéry, D., and Osborne, J. L. Searching for nests of the invasive Asian hornet (Vespa velutina) using radio-telemetry. *Communications Biology*, 1(1):88, 2018. doi: 10.1038/s42003-018-0092-9.

Langkilde, T. and Alford, R. A. The tail wags the frog: harmonic radar transponders affect movement behavior in Litoria lesueuri. *Journal of Herpetology*, 36(4):711–715, 2002. doi: 10.2307/1565948.

Le, Q. S., Kim, J., Kim, J., and Son, H. I. Report on work in progress of small insect tracking system using autonomous uav. In *2017 14th International Conference on Ubiquitous Robots and Ambient Intelligence (URAI)*, pages 242–243. IEEE, 2017. doi: 10.1109/URAI.2017.7992722.

Lövei, G. L., Stringer, I. A. N., Devine, C. D., and Cartellieri, M. Harmonic radar-a method using inexpensive tags to study invertebrate movement on land. *New Zealand Journal of Ecology*, pages 187–193, 1997.

Milanesio, D., Saccani, M., Maggiora, R., Laurino, D., and Porporato, M. Design of an harmonic radar for the tracking of the asian yellow-legged hornet. *Ecology and evolution*, 6(7):2170–2178, 2016. doi: 10.1002/ece3.2011.

Noutahi, E. Fisher's exact test for MxN contingency table. 2018. doi: 10.5281/zenodo.2587757.

Nunes-Silva, P., Hrncir, M., Guimarães, J. T. F., Arruda, H., Costa, L., Pessin, G., Siqueira, J. O., De Souza, P., and Imperatriz-Fonseca, V. L. Applications of RFID technology on the study of bees. *Insectes sociaux*, 66(1): 15–24, 2019. doi: 10.1007/s00040-018-0660-5.

O'Neal, M. E., Landis, D. A., Rothwell, E., Kempel, L., and Reinhard, D. Tracking insects with harmonic radar: a case study. *American Entomologist*, 50(4):212–218, 2004. doi: 10.1093/ae/50.4.212.

Osborne, J. L., Williams, I. H., Carreck, N. L., Poppy, G. M., Riley, J. R., Smith, A. D., Reynolds, D. R., and Edwards, A. S. Harmonic radar: a new technique for investigating bumblebee and honey bee foraging flight. In *VII International Symposium on Pollination 437*, pages 159–164, 1996. doi: 10.17660/ActaHortic.1997.437.15.

Osborne, J. L., Clark, S. J., Morris, R. J., Williams, I. H., Riley, J. R., Smith, A. D., Reynolds, D. R., and Edwards, A. S. A landscape-scale study of bumble bee foraging range and constancy, using harmonic radar. *Journal of Applied Ecology*, 36(4):519–533, 1999. doi: 10.1046/j.1365-2664.1999.00428.x.

Osborne, J. L., Martin, A. P., Carreck, N. L., Swain, J. L., Knight, M. E., Goulson, D., Hale, R. J., and Sanderson, R. A. Bumblebee flight distances in relation to the forage landscape. *Journal of Animal Ecology*, 77(2):406–415, 2008. doi: 10.1111/j.1365-2656.2007.01333.x.

Piper, R. W. and Compton, S. G. A novel technique for relocating concealed insects. *Ecological Entomology*, 27(2): 251–253, 2002. doi: 10.1046/j.1365-2311.2002.00391.x.

Psychoudakis, D., Moulder, W., Chen, C.-C., Zhu, H., and Volakis, J. L. A portable low-power harmonic radar system and conformal tag for insect tracking. *IEEE Antennas and Wireless Propagation Letters*, 7:444–447, 2008. doi: 10.1109/LAWP.2008.2004512.

Rennison, B. D., Lumsden, W. H. R., and Webb, C. J. Use of reflecting paints for locating tsetse fly at night. *Nature*, 181(4619):1354–1355, 1958. doi: 10.1038/1811354b0.

Reynolds, A. M., Smith, A. D., Reynolds, D. R., Carreck, N. L., and Osborne, J. L. Honeybees perform optimal scale-free searching flights when attempting to locate a food source. *Journal of Experimental Biology*, 210(21): 3763–3770, 2007. doi: 10.1242/jeb.009563.

Riley, J. R. and Edwards, A. S. An investigation of the feasibility of using video equipment to record the plant-to-plant movements of green leafhoppers (Nephotettix spp.) within a rice crop. 1994. doi: 10.1038/1811354b0.

Riley, J. R. and Smith, A. D. Design considerations for an harmonic radar to investigate the flight of insects at low altitude. *Computers and Electronics in Agriculture*, 35(2-3):151–169, 2002. doi: 10.1016/S0168-1699(02)00016-9.

Roland, J., McKinnon, G., Backhouse, C., and Taylor, P. D. Even smaller radar tags on insects. *Nature*, 381(6578): 120–120, 1996. doi: 10.1038/381120a0.

Saville, N. M., Dramstad, W. E., Fry, G. L. A., and Corbet, S. A. Bumblebee movement in a fragmented agricultural landscape. *Agriculture, Ecosystems & Environment*, 61(2-3):145–154, 1997. doi: 10.1016/S0167-8809(96)01100-0.

Schaffer, M. J. *Spatial aspects of bumble bee (Bombus spp. Apidae) foraging in farm landscapes*. PhD thesis, Lincoln University, 1997.

Shearwood, J., Hung, D. M. Y., Palego, C., and Cross, P. Energy harvesting devices for honey bee health monitoring. In *Advanced Materials and Processes for RF and THz Applications (IMWS-AMP), 2017 IEEE MTT-S International Microwave Workshop Series on*, pages 1–3. IEEE, 2017. doi: 10.1109/IMWS-AMP.2017.8247435.

Smith, M. T. lionfish0/retrodetect: Initial release, Aug. 2021a. URL `https://doi.org/10.5281/zenodo.5155306`.

Smith, M. T. lionfish0/bee_track: Initial release, Aug. 2021b. URL `https://doi.org/10.5281/zenodo.5155308`.

Smith, M. T. Data from 'a method for low-cost, low-impact insect tracking using retroreflective tags'. May 2021c. doi: 10.15131/shef.data.14650161.v1.

Spencer, J. L., Gewax, L. J., Keller, J. E., and Miller, J. R. Chemiluminescent tags for tracking insect movement in darkness: application to moth photo-orientation. *The Great Lakes Entomologist*, 30(1 & 2):3, 2017.

STOPVESPA. Project: Life14 nat/it/001128 stopvespa final report on the effectiveness of the harmonic radar. Available at `https://www.vespavelutina.eu/Portals/0/Users/152/52/152/LIFE%20STOPVESPA%20-%20Report%20Finale%20Azione%20D2%20-%20Radar%20armonico.pdf?ver=2019-12-04-110820-007` (accessed 2021/08/19), 2019.

Straw, A. D., Branson, K., Neumann, T. R., and Dickinson, M. H. Multi-camera real-time three-dimensional tracking of multiple flying animals. *Journal of The Royal Society Interface*, 8(56):395–409, 2011. doi: 10.1098/rsif.2010.0230.

Vo-Doan, T. T. and Straw, A. D. Millisecond insect tracking system. *arXiv preprint arXiv:2002.12100*, 2020.

Wilson, P. and Stine, M. Floral constancy in bumble bees: handling efficiency or perceptual conditioning? *Oecologia*, 106(4):493–499, 1996. doi: 10.1007/BF00329707.

Wolf, S., McMahon, D. P., Lim, K. S., Pull, C. D., Clark, S. J., Paxton, R. J., and Osborne, J. L. So near and yet so far: harmonic radar reveals reduced homing ability of nosema infected honeybees. *Plos one*, 9(8):e103989, 2014. doi: 10.1371/journal.pone.0103989.

Zanen, P. O. and Cardé, R. T. Directional control by male gypsy moths of upwind flight along a pheromone plume in three wind speeds. *Journal of Comparative Physiology A*, 184(1):21–35, 1999. doi: 10.1007/s003590050303.

Supplementary Material

Capture and Tagging

A foraging bee is captured using a butterfly net (Watkins & Doncaster), placed in a marking cage (Watkins & Doncaster), with a mesh lid at both ends, and placed in either a freezer or ice box (containing ice and salt) to induce narcosis to enable tagging to take place. A small 12 V, 8 cm computer fan, powered with a 9 V battery, is used to ventilate the marking cage, which we found helped reduce the bee's temperature quickly. Although a widely used approach, we note that issues do exist with immobilising bees using cold (or carbon dioxide, CO_2) (Poissonnier et al., 2015). We were also able to attach a tag without cold or CO_2 using a standard queen marking tube with plunger for the *Bombus terrestris* in the Aerial Platform section later in the supplementary. However, the tube mesh limits us to very small tags and we found it more likely to result in failed tagging.

Hardware Notes

To aid replication we elaborate below on several aspects of the hardware design that we found were necessary for successful operation. Figure S1a illustrates the prototype tracking system.

Choice of camera Initial versions of the system used a consumer compact camera (PowerShot SX210, Canon) in which access to the memory card was controlled by connecting or disconnecting the USB power lines from a raspberry pi. Triggering was via a mechanical actuator and flash control was via decoupling the connected slave-triggered flash. We more recently have been using the MV-CA032-10GM (HIKROBOT) camera successfully (2048×1536).

Flash and power The TT560 has a 35 mm full power guide number of 38 m although was used at 1/16 power. Several other low-cost flashes were also used successfully (including the YN560-II, Yongnuo). The choice of 1/16 was determined empirically while also optimising the exposure duration. It was the point at which a reduced signal to background became apparent. We found somewhat variable brightness in the images however, suggesting either the flash power or the timing of the flash or camera trigger can vary slightly.

Electromagnetic pulse protection Each flash (and its trigger cable) was wrapped in aluminium thermal insulation tape and then electrically insulated with a layer of duct tape. Without this, the electromagnetic pulse from the flash-bulb caused the other flashes to also trigger. This did not matter when using the flashes in a combined approach but was necessary for sequential triggering.
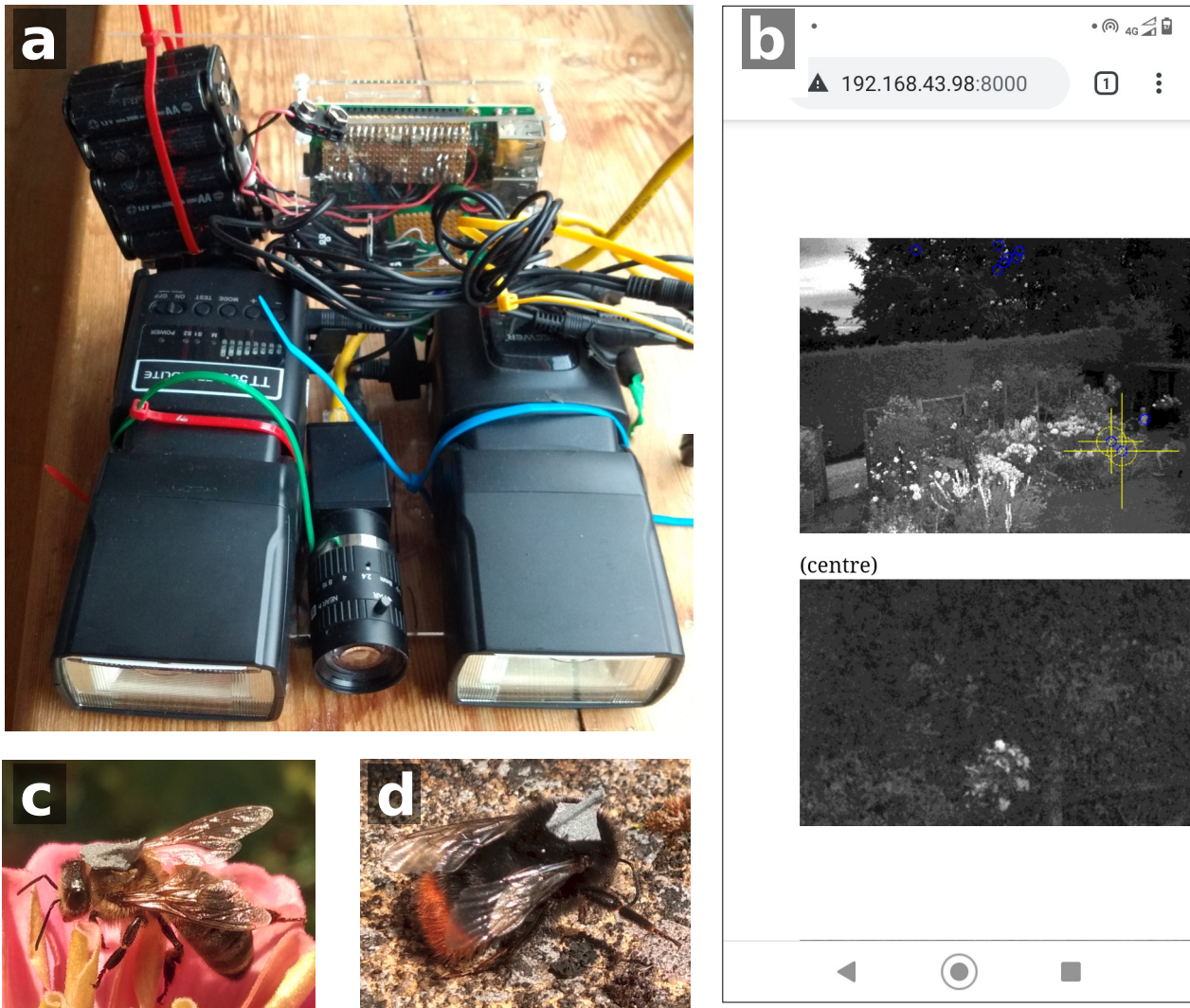
Figure S1: a. The complete tracking system. In the foreground are the two flashes and the camera. Mounted on the back is the raspberry pi and the AA battery packs. b. Screenshot of part of the web interface illustrating real-time target tracking. The yellow crosses with circles are the locations where the system has confidently found the tags. The candidate locations it checked are marked with blue circles (mainly included to support algorithm development). The lower image is simply the central portion of the image, used to ensure the lens is focused (only really necessary after the system's initial construction). c. A tagged *Apis mellifera*, d. A tagged *Bombus lapidarius*.

Filter Earlier in the project we used a near-ultraviolet colour glass filter (50x50 mm, 390 nm Band-pass, Knight Optical) based on the observation that most light impinging our camera will be from foliage, which reflects little light at the blue/violet end of the visible spectrum. However, we found that most false positives and noise were caused by non-foliage objects, so this filtering did not help and also caused an inevitable reduction in signal strength.

Platform For the experiments in this paper we used a simple step ladder or a convenient building to provide elevation. Previously we have explored the use of a 10 m guyed mast (portable folding aluminium telescopic mast, damsu.co.uk), a tethered helium balloon (giant cloudburst chloroprene balloon, balloons.co.uk) and a multirotor UAV. The UAV may have future impact as a method for continuously following the target but has a very limited battery life. The balloon can remain in place longer but can only be used in very calm conditions. The mast is shorter and less flexible but provides stable images allowing more accurate tracking. We would suggest a 2 m or 3 m photography light stand as an ideal platform in future providing a good compromise. Later in the supplementary we describe in more detail the tethered balloon experiments.

Costs A brief note on costs, to emphasise the relative low-cost nature of the system, overall it cost about £820. The electronic-shutter camera and lens were the most expensive components at £630. All other items came to about £190. We are experimenting now with a lower resolution camera (MV-CE013-50GM, HIKROBOT, 1280×960) which costs £205. If this works the unit cost would be about £400. The retroreflectors and glue are almost free (<£0.02/bee).

Software Notes

Other components The implementation of the detection algorithm also checks for broken or skipped frames and, by comparing average brightness, it checks whether the flash has fired or if it has failed (e.g. due to a low flash battery) warns the user. It also looks for large movements (e.g. if the camera is moved) and avoids using images from before the movement in the algorithm above. Finally, in step 4 of the algorithm in Section 2.4.3, rather than compare with all previous images we typically just use images from the last 9 photo-pairs, to save time and memory.

Deployment Two python modules have been written to collect and analyse the camera images in real-time on-board the tracking system. The full code is available to download and use from github.[1] Besides the detection described above, the software also controls the flashes and camera, saves the data to the memory card and can control a servo if mounted on a rotating platform. Finally it provides a web (and API) interface to the system, allowing field-workers to control many aspects of the system (either from a smartphone or laptop). Figure S1b shows an example of the web interface (accessed from a phone). These include the flash configuration and frequency, the detection threshold, etc. The interface also displays the current (and previous) images and targets found (if any) and produces an audio alert on detecting a retroreflector. The system either provides a hotspot or uses a local hotspot (e.g. generated by a smartphone). Other services include high-precision (<2ms error) synchronisation of

---

[1]`https://github.com/lionfish0/bee_track` and `https://github.com/lionfish0/retrodetect`.

3

the datetime onboard using the phone or laptop's clock, so multiple systems used in 3D flight path reconstruction can have accurate datestamps on their images.

Choice of Classifier Given the low number of dimensions and what is likely to be a relatively simple decision boundary, it is likely that most classifiers will perform well. At the time of writing, sklearn (the widely used python library for machine learning) was not easily used with python 3.x on the raspberry pi, and so we used the stand-alone libSVM (Chang and Lin, 2011).

The maximum-dilate operation, $\mathbf{D}_M(\cdot)$

In the algorithm we use the maximum-dilate operation on either non-flash photos $\mathrm{NF}_i^{(j)}$ or on previous subtraction results B_n. The reason is that in both a non-target bright object may have moved a small amount between the two images being subtracted, either due to image misalignment or due to physically moving, e.g. a flower moving in the wind. We still need to ensure this object is 'cancelled' when the one image is subtracted from another. Ideally then we wish to use for subtraction an image (generated by the $\mathrm{D}_M(\cdot)$ function) in which each pixel is the maximum value of all pixels within a certain distance w. Specifically, if $A = \mathrm{D}_M(B)$ then,

$$[A]_p = \max_{q, |q-p|_2 \leq w} [B]_q. \tag{1}$$

Computing this exactly takes a few seconds on the raspberry pi. So for efficiency we compute an approximation. First the image is downscaled by 10 in each direction, but each pixel in the new image is the maximum of the 10×10 grid of original pixels. We then perform the exact calculation, in (1), on this reduced image, before scaling back. This gives a slightly pixelated result to the image being subtracted, but is sufficiently accurate for the system to function.

3D flight path reconstruction

The final experiment used two RTS to compute the flight path of a bee, to demonstrate this as a possible application. After placing the two RTS, nine unique landmarks were identified in the photos from the two systems, and used to place the two cameras in 3D. Specifically, the orientation of the cameras was manually chosen and so was fixed in the model, however the relative positions of the two RTS was optimised inside the model. Ideally the two vectors associated with each landmark should intersect. However aberration, slight mislabelling and other factors can lead to small discrepancies. The model RTSes are placed to minimise the error. The distances between landmarks are known allowing us to calibrate the model.

When accessed through the web interface, the RTS software automatically requests the date and time during initialisation and sets its internal clock. Given the low-latency of the wifi connection to the mobile phone or laptop, the two tracking systems should have a relative accuracy of within 2 ms.

Reconstructing the flight path is not simply a matter of triangulation as the photos are taken at different times. We solve this using a simple approximation in this paper, but describe a more appropriate method for further work in the discussion.

In the field trial, one RTS was the new system capable of 4 acquisitions per second, while the older system only ran every two seconds. So as a simple approach, the old system's vectors are interpolated for each of the new system's. Then the nearest point to these two vectors, that lies equidistant between them, is assumed to be the bee's location.

We finally use these coordinates as training points in three independent Gaussian processes (with the Exponentiated Quadratic kernel), parameterised by time, with appropriate priors regarding plausible acceleration (specifically a lengthscale of 1.5 s was chosen for each axis).

Evaluation

Theoretical Range and Signal

The actual range over which this system could work is difficult to compute as the main source of noise the background landscape and ambient light. One can potentially estimate the relative effectiveness with respect to distance. The apparent size of the reflector will fall by the square of the distance. The light it receives from the flash will also fall by the same. Hence the signal from the reflector will fall proportional to $1/d^4$. Thus if one doubled the camera flash brightness, one would only achieve a 19 per cent increase in range. This relationship is part of the *radar equation*.

We briefly set out a rough sketch of the physics behind the process, to help explain why the reflector is visible. We consider the theoretical potential of the system by considering the proportion of the reflected light that is from the flash compared to the energy from the general background. We do not consider the issue of specular reflections which may result in brighter points than the diffuse light one would normally see in a natural environment. A typical speedlight, taking into account inefficiencies, will release about 2.5 J of visible light energy at 1/16 power over $50\mu s$. We assume approximately the area illuminated by our flash is equal to the distance from the system squared, so if the system is 30 metres from the target the flash will provide 56 Wm^{-2}. At its brightest, sunlight can transmit 445 Wm^{-2} of *visible* light to the Earth's surface. If we use a 3 Megapixel camera covering the same area as the flash, one pixel (from 30 metres) is 3×10^{-4}m^2. We assume the sunlight and flash light will be reflected from the landscape in a diffuse manner, with an albedo of e.g. 0.3, so at the distance of the camera, assuming the light is reflected in all directions equally, the reflection from the background from each pixel will provide a power density of $0.3 \times (3 \times 10^{-4}) \times (445 + 55)/2\pi30^2 = 8.0\mu$Wm^{-2} for that pixel. A 10 mm^2 retroreflector 30 m away will be illuminated by the flash with 556μW. Hawkins et al. (2003) suggest that for a good retroreflector about half the reflected energy is reflected within 0.3 degrees of the entrance angle, which at 30 m will cover an expanse of only 0.1m^2. So will have a power density of $2,814\mu$Wm^{-2}. Thus the pixel with the retroreflector in will return

(training data)		Actual	
		Positive	Negative
Predicted	Positive	90	0
	Negative	14	2,456

(test data)		Actual	
		Positive	Negative
Predicted	Positive	57	1
	Negative	6	1,736

Table S1: Evaluation of the RTS on labelled data. Upper tables when applied to the data used for training. Lower table when applied to new test data (from a different location and day).

		threshold<0		threshold<-1		threshold<-2	
Distance	Flashes	TP rate	FP rate	TP rate	FP rate	TP rate	FP rate
15 m	2	89% (17/19)	5% (1/19)	74% (14/19)	0% (0/19)	47% (9/19)	0% (0/19)
24 m	2	100% (16/16)	0% (0/16)	88% (14/16)	0% (0/16)	88% (14/16)	0% (0/16)
30 m	2	67% (12/18)	17% (3/18)	56% (10/18)	5% (1/18)	33% (6/18)	0% (0/18)
30 m	4	100% (25/25)	12% (3/25)	72% (18/25)	8% (2/25)	68% (17/25)	0% (0/25)
39 m	2	57% (4/7)	57% (4/7)	14% (1/7)	0% (0/7)	0% (0/7)	0% (0/7)
39 m	4	44% (8/18)	17% (3/18)	22% (4/18)	6% (1/18)	6% (1/18)	0% (0/18)

Table S2: Effect of distance and number of flashes on detection rate (TP rate = True Positive rate, FP = False Positive rate). The rate is per image, an image can have both a true positive and a false positive (e.g. if two locations were identified by the tracking system as being a tag). The more negative thresholds are less likely to assign a bright spot a 'positive' target.

hundreds of times more power. It is important to stress that *specular* reflection from litter, metal objects or water can overwhelm this ratio, leading to false positives in the image. Hence the additional processing steps we conduct to remove these artifacts. These calculations show how, in principle, the small reflector can be detected from a considerable distance. We next evaluate the tag empirically to confirm what range is practically possible.

Empirical Range Evaluation

To perform an evaluation we trained the classifier on a smaller subset of the images from one day and location (Site A). We used a small 10 mm^2 tag, realistically what will be visible on a bee. The classifier was used in the pipeline to detect the retroreflector in images from a second day at Site B. The reflector in both was moved between photos at varying locations and distances between approximately 25 m to 40 m away.

Table S1 displays a confusion matrix of the system on the training and test data. Over 90 per cent of the test data points were correctly detected. There was one false positive, upon inspection this was caused by the bright reflection from the watch of a passer-by.

We next reversed the training and test datasets (training using Site B and testing on the data from Site A). The test data samples from Site A had their distances and the use of either two or four flashes recorded. Table S2 illustrates the true and false positive rate, for three choices of classifier threshold. This provides a trade-off between detecting hard-to-spot distant bees, and avoiding false alarms. One might wish to avoid false alarms by using a
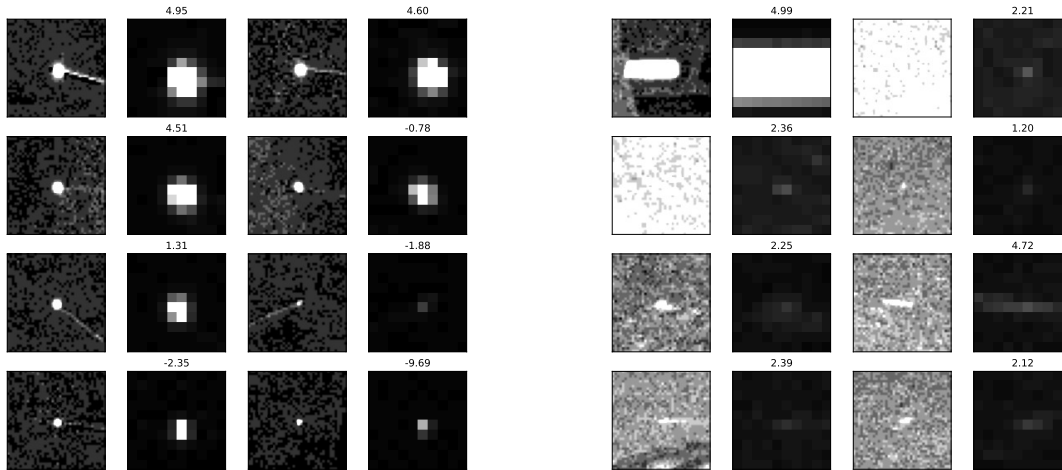
Figure S2: Samples of true (left) and false (right) targets. The first and third column of each are 40×40 greyscale images (white = 5, black = 0) centred on a maximum point. The second and fourth columns are 10×10 enlarged images (white = 50). The value in the title is the classifier score (negative = more confident).

threshold of -2, which in this test data found zero false positives. We found that the RTS worked to approximately 35 m. Obviously the presence or absence of objects that generate false positives, the size of the reflector, the amount of daylight and other factors are also relevant. The sudden loss of signal between 30 and 39 metres relates to the $1/d^4$ relationship with reflected signal strength, the 30 per cent increase in distance equates, in theory, to a 65 per cent reduction in signal strength. We note that in this table and in later field work, where the bee was within 20 m, the classifier did not detect the bee, as it appeared 'too bright'. Some of the plots in Figure S2 demonstrate this. Relatively little training data included samples with this proximity. Provisioning additional, more varied training data will likely solve this. In our case we used an additional threshold heuristic for these very bright spots.

Aerial (tethered balloon) Platform

An early version of the RTS was deployed in September 2018 using a tethered balloon (see Figure S3b) at approximately 15 m above the ground, to test the use of an aerial platform. This experiment was conducted at Site C. We first tagged a *Bombus terrestris* male, found on a *Heuchera villosa*. We released the bee on the same plant. After a period of feeding it left. Within an hour it was detected returning to the plants. Figure S3a illustrates the detection and tracking. It was first detected above the field (at 13:12:32). It was then detected in the planting area (at 13:13:51 and every four seconds after[2]). To confirm the tracked object was real and our tagged bee, we visited the location identified by the system and found the tagged bee (figure S3c) feeding on a *Sedum telephium* not far

---

[2]The delay prior to this second detection was due to users infrequently attending the real-time imagery. The system at this stage did not produce a sound when a detection occured.
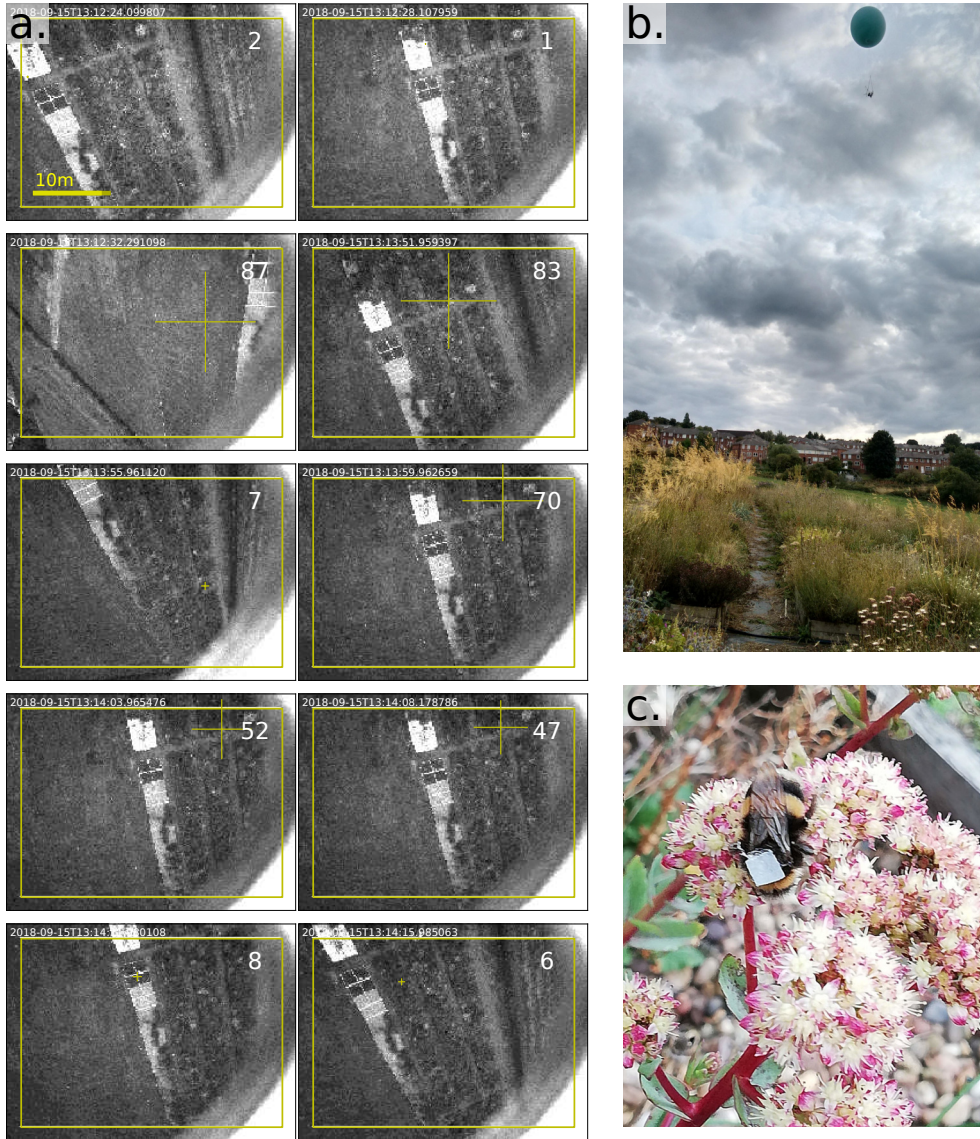
Figure S3: a. Tracking tagged *Bombus terrestris*. Score displayed in top right of each image (over 25 indicates a confident detection). Cross-hair size scaled by score. A returning tagged bee detected as it flew across field (second row, left column) and settled in the planting (second row onwards). Due to wind the camera was at a problematic angle in some of the images. b. The tracking system suspended from the tethered helium balloon. c. The tagged bee, rediscovered using the tracking system. Note: The earlier reflectors were simple flat squares.

from the plant upon which it was released. This provided the first demonstration that the system could detect and track a bee.

The balloon platform was found to be unstable in even slight wind, so in 2019 and 2020, ground based platforms were used with an additional 'ridge' added to the tags to ensure they remained visible from a lower elevation. The view from the balloon platform did make it easier to localise the bee.

Effect of Tags

An important question, when applying novel tags or labels to animals for tracking, is to determine what effect the tags have on behaviour and survival.

Our tags weigh approximately 5 mg, which is at the smaller end of the passive radio tag range - Osborne et al. (1999) used harmonic radar tags weighing 12 mg. Other attempts vary between 1 - 20 mg (Kissling et al., 2014). Importantly though our tags do not require an aerial. In Osborne et al. (1999) the aerial extends 16 mm and some concern is expressed about the effect of the aerial on behaviour. The 5 mg tag compares favourably to the weight of *B. terrestris* workers at 68 to 754 mg (Goulson et al., 2002). Smaller tags were used with *Apis mellifera* workers which are considerably smaller, between 51 and 209 mg (Kaftanoglu et al., 2011) so the tag was still less than 10 per cent of the insect's weight. Figure S1c shows a tagged *Apis mellifera* worker.

Anecdotally, we noted that, immediately after tagging, the bees would often spend a few minutes grooming. Later, all the re-observed insects appeared to return to 'normal' behaviour and would be seen foraging.

The most serious issue with the tags was associated with the artificial nests of *B. terrestris* colonies (Biobest, standard hive). The ridge on the tags would very frequently become entangled in the cotton-wool provided within the hive for thermal insulation. We found the non-cotton-wool nest performed better (although may only be suitable for the warmest parts of the year). One might also consider reducing or avoiding the ridge but this will reduce the signal and range of the system. Conversely we saw several tagged *wild* bees foraging a week after tagging, suggesting that wild bees did not have such issues in their own nests (which do not contain cotton wool).

For a more quantitative assessment of tag effect we followed a similar approach to Hagen et al. (2011), comparing the time spent foraging of tagged and untagged bees. Our experiment was rather less powerful however, as we just looked at foraging time on the flower patch (which probably varies more, especially as we looked at multiple flower types) and we only recorded from when the bee is first seen. In detail: An observer arrived near the forage patch, selected a bee and recorded the time the bee remained foraging before leaving the flower patch (recording also the species and caste of bee, plant and whether the bee had a tag). This introduced (unbiased) additional noise to the data, as the length of the entire foraging session was not recorded. The observer preferentially selected tagged bees, to ensure a roughly balanced dataset. Overall 21 tagged and 19 untagged bees were recorded (respectively 9 and 6 of these were *B. terrestris*, 7 and 2 of these were *B. lapidarius*, other species had fewer samples). Considerable variation in foraging times was present (with times recorded between 6 and 509 seconds). The samples were recorded

at two field sites. To further increase the number of samples we would suggest more field sites should be included so that the same bees were not being repeatedly sampled (which could artificially inflate significance, for example if one individual happened to be very slow or fast).

Hagen et al. (2011, figure 2b) found a significant, 4 fold increase in foraging time for the tagged bees. We did not find any significant difference between the two groups (using either Mann Whitney U or a t-test on the log-times) either within species (e.g. *B. terrestris*.: r = 21 [p = 0.52] t = 0.75 [p = 0.46], *B. lapidarius*: r = 4 [p = 0.46] t = 1.11 [p = 0.30]) or pooled (r = 146 [p = 0.15] t = 1.58 [p = 0.12]). Exponentiating the 95 per cent confidence interval for the difference in log times Tagged/Untagged pooled: [0.85 - 3.66], which compares favourably to tags used in Hagen et al. (2011), although our sample size is small. We also split the data by flower species, and considered both separate species and pooled, but found no significant differences between the tagged and untagged bees, in any of these tests (no correction was made for these multiple comparisons).

List of Authorities

Apis mellifera	Linnaeus, 1758
Megachile sp.	Latreille, 1802
Bombus lapidarius	Linnaeus, 1758
Bombus terrestris	Linnaeus, 1758
Bombus terrestris subsp. *audax*	Harris, 1776
Bombus spp.	Latreille, 1802
Bombus hortorum	Linnaeus, 1761

References

Chang, C.-C. and Lin, C.-J. LIBSVM: A library for support vector machines. *ACM Transactions on Intelligent Systems and Technology*, 2:27:1–27:27, 2011. doi: 10.1145/1961189.1961199. Software available at `http://www.csie.ntu.edu.tw/~cjlin/libsvm`.

Goulson, D., Peat, J., Stout, J. C., Tucker, J., Darvill, B., Derwent, L. C., and Hughes, W. O. H. Can alloethism in workers of the bumblebee, Bombus terrestris, be explained in terms of foraging efficiency? *Animal Behaviour*, 64 (1):123–130, 2002. doi: 10.1006/anbe.2002.3041.

Hagen, M., Wikelski, M., and Kissling, W. D. Space use of bumblebees (Bombus spp.) revealed by radio-tracking. *PloS one*, 6(5):e19997, 2011. doi: 10.1371/journal.pone.0019997.

Hawkins, H. G., Carlson, P. J., Schertz, G. F., and Opiela, K. S. Workshops on nighttime visibility of traffic signs: Summary of workshop findings. 2003.

Kaftanoglu, O., Linksvayer, T. A., and Page Jr, R. E. Rearing honey bees, Apis mellifera, in vitro i: Effects of sugar concentrations on survival and development. *Journal of Insect Science*, 11(1):96, 2011. doi: 10.1673/031.011.9601.

Kissling, W. D., Pattemore, D. E., and Hagen, M. Challenges and prospects in the telemetry of insects. *Biological Reviews*, 89(3):511–530, 2014. doi: 10.1111/brv.12065.

Osborne, J. L., Clark, S. J., Morris, R. J., Williams, I. H., Riley, J. R., Smith, A. D., Reynolds, D. R., and Edwards, A. S. A landscape-scale study of bumble bee foraging range and constancy, using harmonic radar. *Journal of Applied Ecology*, 36(4):519–533, 1999. doi: 10.1046/j.1365-2664.1999.00428.x.

Poissonnier, L.-A., Jackson, A. L., and Tanner, C. J. Cold and CO2 narcosis have long-lasting and dissimilar effects on Bombus terrestris. *Insectes Sociaux*, 62(3):291–298, 2015. doi: 10.1007/s00040-015-0404-8.